AgRISTARS

EW-L1-04134
JSC-17413

A Joint Program for Agriculture and Resources Inventory Surveys Through Aerospace Remote Sensing

October 1981

Early Warning and Crop Condition Assessment

A LOOK AT THE COMMONLY USED LANDSAT VEGETATION INDICES

G. E. Miller

Lockheed Engineering and Management Services Company, Inc.
1830 NASA Road 1, Houston, Texas 77058

Lyndon B. Johnson Space Center
Houston, Texas 77058

1. Report No.	2. Government Accession No.	3. Recipient's Catalog No.
EW-L1-04134; JSC-17413		

4. Title and Subtitle
A Look at the Commonly Used Landsat Vegetation Indices

5. Report Date
October 1981

6. Performing Organization Code

7. Author(s)
G. E. Miller

8. Performing Organization Report No.
LEMSCU-16844

9. Performing Organization Name and Address
Lockheed Engineering and Management Services Company, I c.
1830 NASA Road 1
Houston, Texas 77058

10. Work Unit No.

11. Contract or Grant No.
NAS 9-15800

12. Sponsoring Agency Name and Address
Early Warning/Crop Condition Assessment Project Office
U.S. Department of Agriculture, 1050 Bay Area Blvd.,
Houston, Texas 77058 Technical Monitor: G. U. Boatwr ght

13. Type of Report and Period Covered
Technical Report

14. Sponsoring Agency Code

15. Supplementary Notes
The Agriculture and Resources Inventory Surveys Through Aeros ce Remote Sensing is a joint program of the U.S. Department of Agriculture, the National Aeronautic and Space Administration, the National Oceanic and Atmospheric Administration (U.S. Department of Cor erce), the Agency for International Development (U.S. Department of State), and the U.S. Departme of the Interior.

16. Abstract
This document presents the more common vegetative indic s used with Landsat remotely sensed data and describe their origins, development, logic, an relationships to ground-based measurements of vegetation. The report serves as a lit ature review. An effort has been made to preserve the order in which the various vegetat ve indices appeared in the literature in order to historically trace their underly ig concepts and development.

17. Key Words (Suggested by Author(s))	18. Distribu n Statement
Vegetation Index Numbers, VIN Landsat data	

19. Security Classif. (of this report)	20. Security Classif. (of this page)	21. No. of Pages	22. Price*
Unclassified	Unclassified	36	

*For sale by the National Technical Information Service, ringfield, Virginia 22161

EW-L1-04134
JSC-17413

A LOOK AT THE COMMONLY USED LANDSAT VEGETATION INDICES

Job Order 72-466

This report describes the more common vegetative indices used with remotely sensed data.

PREPARED BY

G. E. Miller

APPROVED BY

USDA

G. O. Boatwright, Manager
Early Warning/Crop Condition
Assessment Project, AgRISTARS
Program

LOCKHEED

J. K. Oney, Project Manager
Early Warning/Crop Condition
Assessment Project Office
Crop Applications Department

LOCKHEED ENGINEERING AND MANAGEMENT SERVICES COMPANY, INC.

Under Contract NAS 9-15800

Earth Resources Applications Division
Space and Life Sciences Directorate
NATIONAL AERONAUTICS AND SPACE ADMINISTRATION
LYNDON B. JOHNSON SPACE CENTER
HOUSTON, TEXAS

October 1981

LEMSCO-16844

CONTENTS

1. INTRODUCTION

1.1 BACKGROUND

The objective of this paper is to present the more common vegetative indices used with Landsat remotely sensed data and describe their origins, development, logic, and relationships to ground-based measurements of vegetation. An effort has been made to preserve the order in which the various vegetative indices appeared in the literature in order to historically trace their underlying concepts and development. A brief discussion of remote sensing preprocessing techniques as input to the vegetation indices is also included.

A vegetative index is simply a formula that transforms the four-dimensional Landsat data into a single real number. This number, the vegetative index number (VIN), may be the reflective count of a single Landsat band, or more commonly a combination of reflective counts of 2 or more bands. In general, the greener and denser the vegetation is in an area, the higher the VIN. The idea has been to formulate VINs that can be used to predict general crop health, crop growth stages, and crop yield.

Since VINs are computed using reflection measurements of one or more Landsat bands, some discussion of the Landsat bands follows. Landsat is a multispectral remote sensing satellite which receives and records reflectance in four spectral bands or channels. The wavelengths and spectrum of these four bands are presented below:

	Wavelength, μm	Spectrum
CH1 = Band 4	0.5 to 0.6	Visible green
CH2 = Band 5	0.6 to 0.7	Visible red
CH3 = Band 6	0.7 to 0.8	Near-Infrared
CH4 = Band 7	0.8 to 1.1	Near-Infrared

Bands 4 and 5 are called the visible bands, and these two bands generally have low reflectance values where there is live green vegetation, particularly band 5. Bands 6 and 7 are the infrared bands, and have high reflectance values where there is live green vegetation. Bauer (ref. 5, page 5) summarizes the reasons for this very concisely: "The low reflectance and transmittance of visible radiation is attributed to the high absorption by leaf pigments, primarily the chlorophylls. However, these pigments are highly transparent to infrared radiation, and the internal cellular structure of the leaf appears to determine the high reflectance at these wavelengths." As a matter of fact, it is known that vegetation reflects more in the near-infrared bands than do most other natural objects (ref. 7, page 2-2), making the near-infrared bands apparent immediate indicators of areas of vegetation, percent ground cover, and biomass. Landsat satellites up to this time have not recorded reflectance below .5 μm or above 1.1 μm, a fact which limits research in some important areas of stress (see section 3.2).

Some further properties of both individual leaf reflectance and crop canopy reflectance which are useful for the Landsat user to know are below, and are taken directly from Bauer (ref. 5, page 5-6). For individual leafs, other important factors affecting reflectance are maturation, senescence, water content, nutrient stress, disease, and insect infestation. In general, as leaves mature, reflectance decreases in the visible spectrum and increases in the infrared spectrum. On the other hand, senescence produces the exact opposite reflectance responses. Both visible and infrared spectral reflectance increases as leaf water content decreases; however, changes in reflectance are not substantial until the leaves reach about 75 percent turgidity. Thus, the change in reflectance is not a sensitive indicator for initial stages of drought. Nutrient stress affects reflectance in both the visible and infrared wavelengths, but increases or decreases in reflectance are dependent upon the type of nutrient stress (see section 3.2). Disease and insect infestation are also known to affect reflectance; however, the wavebands which are necessary for specific detection of these problems on a large scale are restrictive to the extent to keep this area mostly descriptive (see ref. 7, page 4-4; ref. 9, page 1160).

When changing from individual leaf spectral measurements to larger area remotely sensed crop canopies, new variables arise which must be considered:

1. Variations in amount of leaf area, biomass, and ground cover due to differences in planting date, soil type, soil moisture, plant population, and/or disease conditions.
2. Variations in maturity due to differences in variety, planting date, soil type, and soil moisture.
3. Differences in cultural practices, such as tillage or harvesting.
4. Geometric configuration of the crop due to differences in row width, row direction, or lodging of plants.
5. Environmental variables, such as atmospheric conditions, wind, angle of reflection in relation to solar incidence angle, and soil moisture conditions.

Part II of this paper details the mathematical derivations of a number of VINs used today and involved in this is some basic logic or VIN theory. In all derivations, a few basic facts provide much of the background reasoning which will be briefly summarized from Tappan (ref. 19, pages 18-20). The wavelength of .68 is a very good single wavelength to discriminate between living vegetation and dead or dormant vegetation when using wavelengths between 0.4 and 1.1 μm such as Landsat does. Generally, the dead or dormant vegetation has higher reflectance than the living vegetation in the visible portion of the spectrum and lower reflectance in the near-infrared portion. The .68 wavelength also appears to discriminate well between soil and living vegetation, although in this case the optimum wavelength has been found to vary from environment to environment. Living vegetation has minimum reflectance values in the .35 to .5 and .67 to .69 μm ranges, and maximum reflectance values in the .8 to 1.1 range. Referring back to page 1 at the chart on Landsat bands, it is seen that Channel 2 (or Band 5) contains the important .67 - .69 μm range, and that Channel 4 (or Band 7) contains the .8 - 1.1 μm range.

As mentioned earlier, most VINs used today involve combinations of Landsat bands rather than single Landsat bands. It is often hoped that a particular combination of bands will yield more information than can be discerned from individual band values. Multiband VINs tend to be more stable, and thus provide better capability for season to season comparisons of vegetation amounts and conditions (ref. 14, page 1550). Tappan (ref. 19, page 27) gives another important advantage of using multiband VINs rather than single band VINs: in many cases it reduces the amount of "noise" in the Landsat system. Factors such as changes in atmospheric conditions between images taken at different times of the year, attenuation effects due to clouds and haze, topography, shadow, soil and dead vegetation and others may affect all four Landsat bands in either similar or dissimilar ways, but in many cases a band ratio or normalized band combination will result in the partial reduction in the noise, sometimes almost complete reduction.

In summary, VINs are used to clarify information content of Landsat bands for a defined purpose. Purposes of interest include (1) estimates of biomass, leaf area index, density of ground cover and plant height; (2) identification of stressed areas and stress factors; and (3) general and specific crop identification.

1.2 PREPROCESSING OF LANDSAT DATA

It was mentioned in the introduction that Landsat data is altered by sun angle differences, clouds and haze, shadow, and other factors. Some researchers have given attention to the idea of preprocessing Landsat data to reduce the effects of these factors before making use of the data. As previously mentioned, a band ratio or normalized band combination will often result in the partial or almost complete reduction in sun angle or noise factor effects without requiring preprocessing. Nevertheless, it is obviously desirable to have data which contains as little noise as possible before being used in any sense. Some of the preprocessing techniques are given below.

The cosine sun angle correction algorithm (ref. 12, page 718) is a mathematics transformation which corrects Landsat data to a reference solar elevation angle. The correction is applied as follows:

Let X_i = Landsat signal in band i, θ = solar zenith angle, θ_o = reference solar zenith angle, and X_i' = the corrected Landsat band i signal.

Then

$$X_i' = \frac{\cos \theta_o}{\cos \theta} X_i$$

All resulting data will appear to have been acquired at the reference solar zenith angle.

The XSTAR haze correction procedure, developed by Lambeck (ref. 12, page 718; ref. 8, pages 40-43), is a haze correction procedure which has been undergoing revision since 1977. The first version, now known as the global XSTAR procedure (ref. 12), is an algorithm which can be easily applied to Landsat data. However, it has generally been replaced in favor of the new spatially-varying XSTAR procedure (ref. 8). The spatially-varying XSTAR procedure is a multi-step software procedure, and program products from it, along with information about the software, are available from ERIM (Ann Arbor, Michigan).

J. Potter (ref. 15) developed the Atmosphere Correction (ATCOR) program in 1977 to correct Landsat data for haze, sun angle, and background reflectance. The program logic is based, in parts, on principles of radiation transfer theory. The program is available for use at the LARS computation center (West Lafayette, Indiana) and at the NASA JSC Bldg. J17 Computation Center (Houston, Texas). Information concerning the use of ATCOR may be obtained by contacting Lockheed Engineering and Management Services Co. (Houston, Texas).

In summary, it should be noted that none of the development of the VINs presented in this paper considered preprocessing procedures, and as a matter of fact, some VINs had noise reduction included in their development. Of course, any band ratio VIN implicitly corrects for sun angle due to cancellation in the division (ref. 7, page 3-2).

2. CONCEPTUAL AND MATHEMATICAL DERIVATIONS OF VINs

2.1 PEARSON'S AND MILLER'S MULTIBAND VINs

Although single band values from Landsat can be considered VINs, many researchers refer to single band VINs as simply single band values and only regard multiband VINs as true VINs. The rest of this paper will generally follow this outlook. The pioneers of VINs in this context are Pearson and Miller, in 1971, and since then many VINs have been formulated.

Pearson and Miller conducted extensive studies in 1971-72 on vegetation canopy reflectance using grass plots (ref. 14; ref. 19, page 21 for summary of their findings) and among other conclusions chose .68 μm and .78 μm as the two optimal wavelengths for separating green vegetation from soil and dead or dormant vegetation. Figure 1 is a copy from page 1362 of ref. 14 of a graph which shows the reflectance curves of soil, dead or dormant vegetation, and live green vegetation superimposed for what was considered a typical short grass prairie plot. They also found that an inverse linear correlation existed between reflectance and green vegetation at .68 μm, and a direct linear correlation existed between reflectance and green vegetation at .78 μm. Going further, they found that using combinations of the reflectance of these two wavelengths yielded even higher correlations between reflectance and total biomass (live and dead biomass) _ sometimes $r > 0.90$. First, they correlated total biomass with .78 μm minus .68 μm reflectance values and obtained an $r = .88$; an $r = .91$ was obtained when they correlated total biomass with the ratio of the reflectance at .78 μm to that at .68 μm. The underlying principle in both cases is that as the quantity of green vegetation increases in a given area, the red wavelength (.6 to .74 μm) reflectance decreases whereas the near-infrared wavelength (.74 to 1.35 μm) reflectance increases. This same principle is used in many of the subsequent VINs which quickly followed, many of which are still used today.

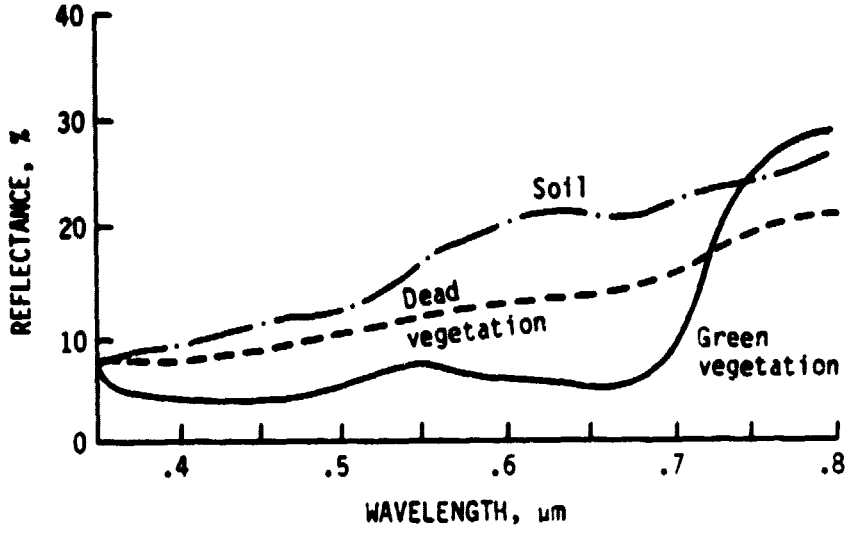

Figure 1.- Typical wavelength versus reflectance curves (Source: ref. 14, p. 1362).

2.2 DEVELOPMENT OF THE TVI

As part of the Great Plains Corrider Rangeland Project conducted at Texas A&M University, Rouse et al. (ref. 17) in 1973 developed a VIN which they called the Transformed Vegetation Index (TVI). It uses the basic theory developed only a year or two earlier by Pearson and Miller: that a contrast between the .78 and .68 μm wavelengths provided a better correlation with biomass than did single wavelengths.

The work carried on in this project was some of the first to use Landsat data. Since Landsat does not have individual spectral wavelengths (such as .68 μm and .78 μm) but rather wavebands, Rouse and others use bands 5 and 7 (or channels 2 and 4) to correspond with the wavelengths .68 and .78 μm respectively. The contrast used was the spectral value of channel 4 minus the spectral value of channel 2. Sun angle and haze were seen to be a problem, and a normalization procedure was used to eliminate the effects as much as possible: dividing the contrast of the two channels by the sum of the two channels. The addition of 0.5 to this quotient was done to avoid working with negative numbers. Since

they thought that the variance of this result might be proportioned to the mean values, they took the square root of it. The result was named the TVI. The above verbal description of the computation of the TVI is simplified as follows:

$$TVI = \sqrt{\frac{CH4 - CH2}{CH4 + CH2} + 0.5}$$

Further analysis of their data indicated that the TVI was not sensitive to sparsely vegetated areas. However, results of the study also concluded that the TVI was adequate for monitoring the vernal progression and retrogradation of vegetation within the Great Plains Corrider, (ref. 17, page 313), and also had potential for measuring increments in green biomass, useful in regional agricultural applications.

The TVI is often now referred to as the TVI7. The reason for this is that another TVI has been developed, the TVI6, which is the original TVI using Landsat band 6 (channel 3) in place of band 7 (channel 4). Since the important .78 μm wavelength is seen to be bordering bands 6 and 7, the .78 μm - .68 μm contrast can be attained using either band, although some prefer band 7 over band 6 and some vice-versa. In summary, TVI7 and TVI6 are computed as follows:

$$TVI7 = \sqrt{\frac{CH4 - CH2}{CH4 + CH2} + 0.5}$$

$$TVI6 = \sqrt{\frac{CH3 - CH2}{CH3 + CH2} + 0.5}$$

2.3 DEVELOPMENT OF THE AVI

About the same time that Rouse and others were conducting their studies which led to the creation of the TVI, other research was being conducted by P. Ashburn (ref. 3) which led to the creation of the Ashburn Vegetation Index (AVI) in 1974. Ashburn's intention was to provide some measure in green growing vegetation, and the hope was that this measure could be helpful in crop identification studies using VIMs; section 11 of this paper reports on the use of the AVI toward this goal.

Like the TVI, the AVI makes use of the basic theory developed 2 years earlier by Pearson and Miller: that the .78 μm - .68 μm wavelength contrast provides a better greenness measure than do single wavelengths. Using Landsat data, Ashburn set the AVI = 2(CH4) - CH2, where the doubling of channel 4 normalizes the two channels (since CH4 digitizes from 0-63 for black to white and all other channels digitize from 0-127 for black to white). All negative AVI values are set to zero.

Two things about the AVI make its use very desirable in large-scale computer applications. The first is the simplicity of the formula. A simple calculation is very desirable when processing many Landsat segments _ each of which have 22,932 pixels with 4 channels of information. The second is the dichotomous implication which results from AVI computation: a positive AVI signifies at least some growing vegetation in a scene, a zero AVI signifies no growing vegetation. This makes the AVI a favorite for masking applications.

2.4 DEVELOPMENT OF THE GVI, SBI, KVI, AND GIN

In 1976, R. J. Kauth and G. S. Thomas published a paper (ref. 13) the results of which have had great impact on agricultural remote sensing research. In this paper, they outline a transformation which can be applied to Landsat data which preserves four independent dimensions of a Landsat scene. The remainder of this section is devoted to describing the development of this transform and the VINs which result.

Their work began by inspecting scatter plots of 1973 channel 2 versus channel 3 digital values obtained from Landsat 1 over certain Illinois counties (ref. 12, page 705). The scatter plot's values were not the digital values for single Landsat pixels over a segment, but instead were approximate digital values of numerous clusters of Landsat pixels for several segments. For each of these clusters, the exact soil type, vegetation cover, etc. for the actual land areas in each cluster were known.

A shape resembling what Kauth and Thomas called a tasselled cap was seen to be the overall pattern in the scatter plots. Figure 2 displays an actual scatter plot in Illinois and an outlined tasselled cap. It was seen to be a typical scatter plot and used for further study. The clusters along the base of the cap in figure 2 were known by Kauth and Thomas to be varying shades of bare soil. Thus, the base of the cap could be used as a soil brightness line. This soil brightness line is, of course, seen only in two-dimensional space since figure 2 is two-dimensional (channel 2 versus channel 3). The next question is what happens when three dimensions are considered instead of just two? Would the soil brightness line change into a soil brightness plane with an additional Landsatl channel considered, and what additional changes with the fourth channel also considered? When Kauth and Thomas added channel 1 to their scatter plot study of the figure 2 clusters, they found a shape which resembled a tasselled cap in three-dimensional space (this tasselled cap appeared to be one which had not been opened to wear — it was still basically planar but not completely). Figure 3 is a resemblance of the three-dimensional (channel 1 versus channel 2 versus channel 3) tasselled cap. Because of the small "thickness" channel 1 added to the tasselled cap representation, a thin cigar-shaped plane of soils resulted in the three-dimensional plots; this resulted in Kauth and Thomas continue to think in terms of a basic line of soils, even in the three-dimensional space (see fig. 3). The last channel, channel 4, was found to have an almost identical graphical effect to that of Channel 1.

With the various scatter plots described above, Kauth and Thomas were now able to describe a line of soils in four-channel space. This is done by connecting the point (0, 0, 0, 0) to the point R_1 (in Figure 3), where R_1 is obtained, of course, from looking at the numerous scatter plots that had been created, (even though R_1 in fig. 3 is only shown in its three-dimensional space). The description of this line of soils is simply a vector, or soil brightness vector. As a unit vector, the soil brightness vector is described as follows:

$$.433(CH1) + .633(CH2) + .586(CH3) + .264(CH4)$$

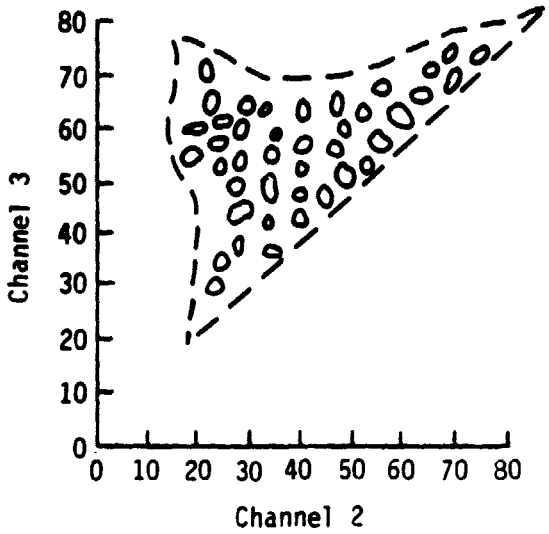

Figure 2.- Cluster patterns from Fayette County, Illinois, June 11, 1973 (Source: ref. 13, p. 4B-47).

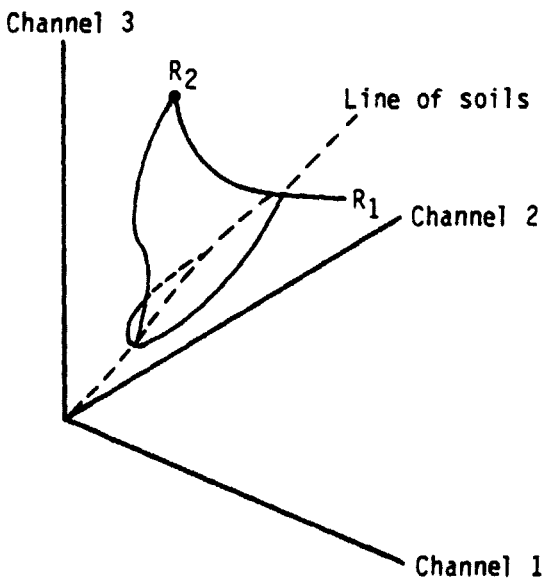

Figure 3.- Three-dimensional Tasselled Cap representation (Source: ref. 12, p. 707).

For any pixel, a soil brightness measure could be obtained by using the above soil brightness unit vector with the CH1 - CH4 digital values of that pixel. This soil brightness measure is now called the Soil Brightness Index (SBI), and as seen from above,

$$SBI = .433(CH1) + .633(CH2) + .586(CH3) + .264(CH4)$$

At this point, Kauth and Thomas reexamined the tasselled cap scatter plots and noted that the clusters which contained pixels having high greenness or living vegetation appeared toward the top of the tasselled cap. The farther the cluster was from the line of soils of figure 3, the more vegetation or greenness in that cluster. Thus, they created a new vector pointing in a perpendicular direction from the line of soils to R_2; this vector was actually generated by using the Gram-Schmidt orthogonalization procedure and was also made into a unit vector. This vector, which is obviously considered to be a measure of greenness, is described as follows:

$$-.290(CH1) - .562(CH2) + .600(CH3) + .491(CH4)$$

For any pixel, a greenness measure could be obtained by using the above greenness vector with the CH1 - CH4 digital values of that pixel. This greenness measure is now called the Green Vegetation Index (GVI), and as seen from above,

$$GVI = -.290(CH1) - .562(CH2) + .600(CH3) + .491(CH4)$$

Figure 2 clusters which were not soil but did not contain pixels having high greenness but instead contained what was called yellow stuff were selected, (actually fig. 2 did not contain any yellow pixels, and these had to be simulated from other scatter plots). Using Gram-Schmidt again, Kauth and Thomas created a new "yellow" vector which is orthogonal to both the soil brightness and greenness vectors. As a unit vector, this vector is described as follows:

$$-.829(CH1) + .522(CH2) - .039(CH3) - .194(CH4)$$

For purposes of finishing a matrix described later, and to describe a fourth factor which cannot be defined as soil brightness, greenness, or yellowness, a fourth vector was created, and was said to be a feature of "none-such" or "none of the above factors". It is simply a vector chosen to be orthogonal to the above 3 vectors, and was created by Gram-Schmidt again. As a unit vector, this "none-such" vector is described as follows:

$$.223(CH1) + .012(CH2) - .543(CH3) + .810(CH4)$$

Using the four vectors above, it was now possible to define four independent factor measures for any pixel, even though it is accepted that only the first two vectors provide meaningful information. Rather than using the vectors totally independent of each other, Kauth's and Thomas' whole ingenious system can be explained completely in terms of a single transformation, which Kauth and Thomas outline (ref. 13, page 48-43) as follows:

Let $u = R^T X + r$

where x is the Landsat MSS signal vector expressed in counts

u is the transformed vector, also expressed in counts

r is an arbitrary offset vector, simply introduced to avoid negative values in u

R is a unitary matrix, whose columns are simply the aforementioned unit vectors of soil brightness, greenness, yellowness, and none-such respectively.

In much of the literature, the whole transformation system is explained as a multiplication of a rotation matrix by CH1 - CH4 _ this is, in essence, the case. This rotation matrix, often called K, is equal to R^T,

$$K = R^T = \begin{pmatrix} .433 & .633 & .586 & .264 \\ -.290 & -.562 & .600 & .491 \\ -.829 & .522 & -.039 & .194 \\ .223 & .013 & -.543 & .809 \end{pmatrix}$$

and CH1 - CH4 multiplied by the first row equals the SBI, CH1 - CH4 multiplied by the second row equals the GVI, CH1 - CH4 multiplied by the third row is a yellow number, and CH1 - CH4 multiplied by the fourth row is a none-such number. As mentioned before, the SBI and the GVI are the only measures of interest in most cases. Figure 4 shows how SBI and GVI may be viewed graphically in three-dimensional space.

Often in the literature, especially since LACIE, a different Kauth rotation matrix is seen. The K rotation matrix shown above was the matrix derived by Kauth and Thomas using Landsat 1 data only. Landsat 2 and 3 have since been launched, and due to sensor calibration differences, modified K matrices have had to be developed, although they serve the exact same purpose. When using Landsat 2 digital values, which currently is the standard, the following rotation matrix is used:

$$K = \begin{pmatrix} .332 & .603 & .676 & .263 \\ -.283 & -.660 & .577 & .388 \\ -.900 & .428 & .076 & -.041 \\ -.016 & .131 & -.452 & .882 \end{pmatrix}$$

When using Landsat 3 digital values, the following rotation matrix is used:

$$K = \begin{pmatrix} .386 & .742 & .842 & .279 \\ -.329 & -.812 & .719 & .412 \\ -1.044 & .527 & .095 & -.043 \\ -.019 & .161 & -.563 & .937 \end{pmatrix}$$

Again, CH1 - CH4 multiplied by the first row equals the SBI, etc., just as before. Interestingly enough, the methods used in creating the rotation matrices for Landsat 2 and 3 data were not the exact same methods used by Kauth and Thomas in creating the rotation matrix for Landsat 1 data, although they could have been. Since the basic purpose of Part II of this paper is to present the concepts and mathematics of the original developmental work done on various VINs, the differences in the methods that Kauth and Thomas used to create the Landsat 1 data rotation matrix and the methods used to create the rotation matrices used with Landsat 2 and 3 data will not be presented here, except very briefly below. The rows of the rotation matrix K for use with Landat 2 are transposed unit vectors characterizing Landsat 2 data rotation

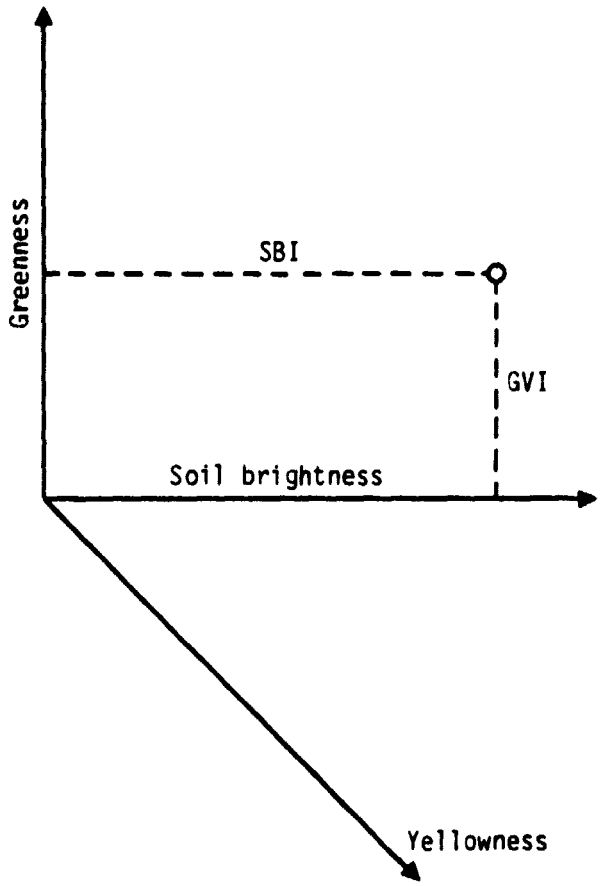

Figure 4.- A graphical view of the orthogonal relationship between the SBI and the GVI (Source: ref. 10, p. 8).

into Tasselled cap data space particularly oriented to suit Lambeck's XSTAR algorithm (ref. 12, page 717--this reference also provides other references into the exact methodology used). Rows 1 through 4 of rotation matrix K for use with Landsat 2 are simply multiplied by 1.161, 1.230, 1.246, and 1.062 respectively (calibration difference adjustments) to obtain the four rows of the rotation matrix for use with Landsat 3 data (ref. 8, page 2).

The most common use of the Tasselled Cap Transformation system is a pixel scatter plot of GVI versus SBI, where GVI is the vertical axis and SBI is the horizontal axis, (ref. 7, page 3-5). Using this scatter plot, a horizontal line is drawn below which are approximately one percent of the pixels. This line or value is called the soil line (getting rid of the bottom one percent is thought to protect against swampy areas and low outliers). Subtracting the soil line value from the GVI yields a result called the Green Number, or sometimes called the Kauth Vegetation Index (KVI). As a formula, the Green Number, or KVI, is represented as follows:

$$KVI = GVI - (\text{Soil Line Calculation})$$

Any pixel having KVI = 0 should be bare soil, any pixel with KVI > 0 should have some green vegetation, and any pixel having KVI > 15 is considered to be highly green.

In 1977, while studying drought, Thompson and Wehmanen (ref. 20) created the Green Index Number (GIN). The GIN is not considered to be a VIN, since it is not a pixel measurement, but can be thought of as a "segment VIN". The creators defined the GIN to be the percent of pixels in a segment with KVI > 15, (ref. 20, page 203), computed as follows:

$$GIN = \frac{N}{22,932} \times 100$$

where

N = number of pixels with KVI > 15, and 22,932 = number of pixels in a segment.

The GIN may be said to be the percentage of a segment with a nearly full cover of green healthy vegetation.

2.5 DEVELOPMENT OF THE PVI AND DVI

Richardson and Wiegand (ref. 16) conducted research in 1977 with hopes of creating procedures that would account for soil background variations — a factor known to hamper interpretation of vegetation surface reflectance. A year earlier Kauth and Thomas determined that the data space distribution of soil reflectance variation in Landsat data is confined to a line (in two-dimensional data space) or a plane (in three-dimensional data space), and that reflectance variation of developing vegetation grows perpendicularly out of the plane of soils. Using this information, Richardson and Wiegand set about research that would lead to the creation of the perpendicular vegetation index (PVI7, PVI6) and the difference vegetation index (DVI).

First, they obtained Landsat digital counts (in each of the four Landsat bands) from highly reflective bare soil, low reflectance bare soil, cloud tops, cloud shadows, and water on April 2, May 17, June 4, July 10, October 17, and December 10, 1975 in Hidalgo and Willacy counties, Texas (if interested, exact counts are on page 1543, ref. 16). Next, for each pairwise Landsat band combination, a linear regression was run for purposes of determining Kauth's line of soil. A table displaying their results is shown in table 2 (copied from ref. 16, page 1543).

At this point it was determined that it was not necessary to continue their study using all of the MSS band pairwise combinations, and the following logic was used to eliminate all but band combinations (5, 6) and (5, 7): band combinations (4, 5) and (6, 7) were eliminated because bands within the visible and infrared are known to be highly intercorrelated, band combinations (4, 6) and (4, 7) were eliminated because they had lower correlation coefficients and higher standard errors of estimate than did (5, 6) and (5, 7), and finally because band combinations (5, 6) and (5, 7) had been found useful in past studies. The linear equations for these two band combinations were designated as soil background lines, (Note: for (5, 7) the intercept was not statistically significant; thus set to 0).

TABLE 2.- LINEAR EQUATIONS DETERMINING KAUTH'S LINE OF SOIL FOR ALL POSSIBLE PAIRWISE COMBINATIONS OF THE 4 LANDSAT MSS BANDS. DIGITAL COUNT DATA ARE FOR APRIL 2, MAY 17, JUNE 4, JULY 10, OCTOBER 17, AND DECEMBER 10, 1975 FROM HIGH AND LOW REFLECTANCE SOIL, AND CLOUD AND CLOUD SHADOWS (N = 16).

MSS band pairwise combination (X_1, X_2)	Correlation coefficient (r)	Linear equations $X_1 = a_0 + a_1X_2$	Standard error of estimate ($S_{x1 \cdot x2}$)
			Digital counts
(4, 5)	0.967	$X_1 = -1.04 + 0.938X_2$	10
(4, 6)	0.949	$X_1 = -5.45 + 1.011X_2$	12
(4, 7)	0.958	$X_1 = -1.23 + 2.257X_2$	11
(5, 6)	0.993	$X_1 = -5.49 + 1.091X_2$	5
(5, 7)	0.987	$X_1 = -0.01 + 2.400X_2$	6
(6, 7)	0.993	$X_1 = 5.09 + 2.200X_2$	4

Richardson and Wiegand then plotted LAI values from some previously collected sorghum data for comparison with their soil bandground line (using the MSS5 and MSS7 line). They noticed that data points for the sorghum fields deviated perpendicularly from the bare soil background line, and furthermore that the sorghum fields with larger LAI values (denser vegetation) were displaced furthest from the line. They concluded that a measure of the distance of a candidate sorghum point from the line could be used as an index of vegetation amount for that sorghum point. They also noticed that water deviates from the soil background line, but on the opposite side. Using the above findings, they concluded that indeed the soil background line could perhaps serve as a soil background reference for a vegetation index model.

For both the (5, 7) and (5, 6) band combinations, a vegetation index model, or VIN, was created simply using the perpendicular distance of a vegetation

candidate signature point from the soil background line. Each will be treated separately (to prevent confusion), using the notation and descriptions of the originators. For MSS5 and MSS7, this perpendicular distance is given by the equation:

$$PVI7 = \sqrt{(R_{gg}5 - R_p5)^2 + (R_{gg}7 - R_p7)^2}$$

where

PVI7 — is the perpendicular VIN, defined as the perpendicular distance between the candidate vegetation point and the soil background line for Landsat bands MSS5 and MSS7,

R_p — is the reflectance of a candidate vegetation point for MSS5 and MSS7, and

R_{gg} — is the reflectance of soil background corresponding to a candidate vegetation point,

and this distance shall be defined as "positive" if $R_{gg}5 > R_p5$; "zero" if $R_{gg}5 = R_p5$, and "negative" if $R_{gg}5 < R_p5$.

A picture displays this well:

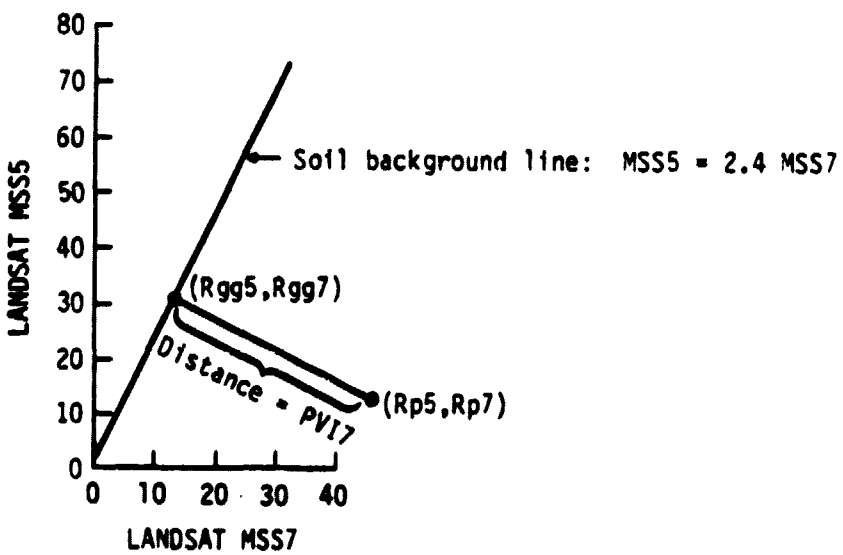

Since the soil background line is known, R_p5 and R_p7 for a candidate vegetation point is known (they are simply the Landsat digital counts for the vegetation point), and the slope of the perpendicular line connecting (R_p5, R_p7) with the soil background line is known (it is always the negative reciprocal of a line slope, in this case -1/2.4 = -.417), all that remains is to solve for $R_{gg}5$ and $R_{gg}7$, which yields:

$$R_{gg}5 = .851\ R_p5 + .355\ R_p7, \text{ and}$$

$$R_{gg}7 = .355\ R_p5 + .148\ R_p7.$$

This, in turn, yields:

$$PVI7 = \sqrt{(R_{gg}5 - R_p5)^2 + (R_{gg}7 - R_p7)^2}$$

$$= \sqrt{[(.850\ R_p5 + .355\ R_p7) - R_p5]^2 + [(.355\ R_p5 + .148\ R_p7) - R_p7)]^2}$$

$$= \sqrt{(-.149\ R_p5 + .355\ R_p7)^2 + (.355\ R_p5 - .852\ R_p7)^2}$$

$$= \sqrt{[.355(CH4) - .149(CH2)]^2 + [.355(CH2) - .852(CH4)]^2}$$

which is the form appearing in most of the literature. Using the above distance formula, and the conclusions from the sorghum studies mentioned earlier, they were also able to conclude that a "positive" PVI7 indicated vegetation, a "zero" PVI7 indicated bare soil, and a "negative" PVI7 indicated water.

Richardson and Wiegand also created a computationally simpler VIN using the soil background line of MSS5 and MSS7. It is simply:

$$DVI = 2.4MSS7 - MSS5$$

$$= 2.4(CH4) - CH2$$

and achieves the same purpose as the PVI7. Just as with the PVI7, a "positive" DVI indicates vegetation, a "zero" DVI indicates bare soil, and a "negative" DVI indicates water. However, with the DVI, the terms negative, zero, and positive have pure mathematical meaning: DVI < 0 indicates water, etc.

However, the DVI has a disadvantage since the soil background coordinates ($R_{gg}5$, $R_{gg}7$) cannot be determined.

Another perpendicular VIN, PVI6, was also created by Richardson and Wiegand. It is computed exactly as PVI7 but uses Landsat bands 5 and 6 instead of bands 5 and 7, and also uses the linear equation associated with bands 5 and 6, (MSS5 = -5.49 + 1.091 MSS6). This yielded:

$$PVI6 = \sqrt{(R_{gg}5 - R_p5)^2 + (R_{gg}6 - R_p6)^2}$$

$$= \vdots$$

$$= \sqrt{[-.498 - .457(CH2) + .498(CH3)]^2 + [2.734 + .498(CH2) - .543(CH3)]^2}$$

Richardson and Wiegand (ref. 16, page 1548) state reasons why they feel that the perpendicular VINs, PVI7 and PVI6, have a fundamental advantage over the other VINs existing at that time, which included the TVI7, TVI6, DVI, GVI, SBI, and any single bands or simple ratio of two bands. Briefly, the PVI7 and PVI6 calculate the soil background intersection coordinates which allow examination of reasons (water content differences, shadows, tillage, soil crusting) for differences in reflectance of cropland, rangeland, and forest scenes due to soil background.

2.6 DEVELOPMENT OF THE LAI

LAI, or leaf area index, is not a VIN but rather an important agronomic variable. Evapotranspiration and photosynthesis models used regularly by researchers use LAI inputs. Also, crop growth models use LAI inputs indirectly, since crop growth models typically include evapotranspiration and photosynthesis subroutines (ref. 21, page 340). Correlation studies completed by Aaronson and Davis (ref. 1) have indicated a relationship between LAI and wheat yield. However, a large problem exists: ground measurements of LAI are very tedious and expensive (and, of course, not possible in many foreign

areas). If LAI could ever be estimated by use of Landsat measurements, the above mentioned uses of LAI could be made much more inexpensively and could also be extended to much larger areas. A few such efforts at LAI estimation have been made, almost exclusively by E. T. Kanemasu working with mostly wheat data.

Standard regression analysis was used to derive estimated LAI models in the known efforts toward LAI estimation, with ground measurements of LAI as the dependent variable and Landsat band ratios or other VINs as the independent variables. Even though LAI itself is not a VIN, model estimated LAI may be thought of as a VIN since it is a number derived completely from Landsat band combinations; thus model estimated LAI has appeared in some VIN comparison studies.

Although a number of LAI formulas have been proposed and used over the last few years, only three will be detailed in this section — one because it was used in a large VIN comparison study (ref. 1) and at the time of this report is still being used by FAS/CCAD in Houston, the others because they are currently accepted as the best wheat LAI estimates. All three are for wheat only since this is where the emphasis has been.

The LAI estimator used by FAS/CCAD during the last few years and by Aaronson and Davis (ref. 1) in their VIN comparison study is:

$$LAI = 41.325 \left(\frac{CH1}{CH2}\right) - 42.45 \left(\frac{CH1}{CH3}\right).$$

Unfortunately, this author has been unable to find a single reference with respect to the original development of this formula (including its originator) or how well the model performed. It does appear similar to some of Kanemasu's earlier formulas; however, Kanemasu disclaims it.

In 1977, Kanemasu (ref. 21, page 339), using many observations taken over a two year period from three large (over 40 ha) Kansas winter wheat fields, developed the following LAI model:

$$(1) \qquad LAI = 2.677 - 3.694\left(\frac{CH1}{CH2}\right) - 2.309\left(\frac{CH1}{CH3}\right) + 5.751\left(\frac{CH1}{2CH4}\right)$$

$$+ .043\left(\frac{CH2}{CH3}\right) - 2.692\left(\frac{CH2}{2CH4}\right) + 3.071\left(\frac{CH1}{CH2} - \frac{CH1}{2CH4}\right)\left(\frac{CH1}{CH2}\right).$$

An $R^2 = .69$ was obtained with this model.

Kanemasu tried to improve the above model by using stepwise regression analysis on 115 observations of LAI and their respective Landsat MSS data (again Kansas winter wheat) and a decision logic based upon low LAI versus high LAI areas (ref. 10, page 10). This resulted in the following model:

$$CLAI = .366 - 2.265\left(\frac{CH1}{CH3}\right) - .431\left(\frac{CH1}{CH2} - \frac{CH1}{CH4}\right)\left(\frac{CH1}{CH2}\right) + 1.745\left(\frac{CH1}{CH2}\right) + .057\,(PVI7);$$

If $CLAI < 0.5$, then

$$LAI = 1.093 - 1.138\left(\frac{CH2}{CH3}\right) - .017\left(\frac{CH1}{CH2} - \frac{CH1}{CH4}\right)\left(\frac{CH1}{CH2}\right) - .016\,(PVI7),$$

else

$$LAI = -5.33 + .036\,(PVI7) + 6.54\,(TVI6).$$

This model yielded an $R^2 = .69$, no improvement over the R^2 of the simpler (1) model.

Before leaving this section, it should be noted that Kanemasu has also produced various estimated LAI formulas for sorghum and soybean (ref. 11, page 46; ref. 21, page 338), however, these appear to be preliminary in nature and not meant for usage.

3. VIN RELATIONSHIPS TO AGRONOMIC VARIABLES

3.1 YIELD AND YIELD COMPONENTS

This section discusses VIN relationships with yield and yield components: percent crop cover, biomass, plant height, leaf area index, and yield.

Richardson and Wiegand (ref. 16) calculated correlation coefficients for the following Landsat bands and VINs with percent crop cover, plant height, and leaf area index for ten sorghum fields: the individual Landsat bands, band 5 divided by band 7 (sometimes called RVI), TVI7, TVI6, PVI7, PVI6, DVI, GVI, and SBI. They found that the individual Landsat bands had the highest correlations with all three agronomic variables. Band 5 was correlated highest with crop cover and plant height ($r = -.809$ and $r = -.849$ respectively), and band 6 was correlated highest with leaf area index ($r = -.849$). The highest VIN correlations were TVI6 with crop cover ($r = .716$), TVI6 with plant height ($r = .828$) and PVI6 with leaf area index ($r = .812$). All the above coefficients were significant at the .01 level except TVI6 with crop cover, which was significant at the .05 level.

Tappan (ref. 19, page 92) found that the simple band ratios and band differences seemed to correlate best with percent green vegetation cover when working with Kansas prairie data. All the simple band ratios and simple band differences he worked with yielded $r > .9$. Tappan also noted (through personal communication) that percent ground cover and biomass have a direct relationship when vegetative ground cover is less than 100%, and therefore the VINs which work well with percent cover also work well with biomass. Once 100% ground cover is reached, band 7 has been found to be useful for detecting changes in biomass (ref. 19, page 25).

Aaronson and Davis did a comparative VIN correlation study (ref. 1) using the AVI, DVI, GVI, KVI, LAI, PVI6, PVI7, TVI6, and TVI7, where LAI in this case is the estimated LAI given by LAI = 41.325 (CH1/CH2) - 42.45 (CH1/CH3) described in section 8. Using winter wheat data, they correlated the VINs with each other, yield, plant height, and biomass at each of the following growth

stages: planting, tillering, stem extension, heading, flowering, ripening, and harvest. Among their major conclusions were:

1. All VINs in the study were highly correlated in each of the growth stages, (see ref. 1, page 10 for growth stage descriptions)
2. The VINs were correlated to yield similarly at each of the growth stages, with highest correlations occurring at heading. LAI and TVI6 had the highest correlations with yield, and at heading had respective correlation coefficients of .64 and .63 (both at .0001 significance).
3. The VINs were correlated to biomass and plant height similarly at tillering and stem extension, with the highest correlations occurring at stem extension. Correlations with biomass at stem extension ranged from r = .65 to r = .71 (all at .0001 significance) for all the VINs with TVI6 ranking highest. Correlations with plant height ranged from .76 to .84 (at .0001) with AVI, DVI, and PVI7 ranking highest.

Kanemasu, as noted in section 8, has been the pioneer in LAI estimation research, particularly for wheat. Some of his earlier estimated LAI models were simply functions of the PVI7 (ref. 21, page 337-338), and even his later two-step LAI model includes the PVI7 and TVI6 (ref. 10, page 10), thus showing the relationship noticed by Kanemasu between VINs and LAI. Working with 115 observations of Kansas wheat data, Kanemasu found the following coefficients of determination between LAI and the below VINs and band ratios (ref. 10, page 11):

VIN	R^2	Band Ratio	R^2
PVI7	.55	CH2/CH3	.56
PVI6	.55	CH2/CH4	.48
TVI7	.50	CH1/CH4	.27
TVI6	.59	CH1/CH3	.20
GVI	.57	CH1/CH2	.10

3.2 STRESS FACTORS

Three common stress factors affecting crop condition are water stress, nutrient deficiencies, and diseased or infested crops. The use of Landsat VINs in detecting these factors is the topic of this section.

Thompson and Wehmanen (ref. 20) successfully used the GIN in operation mode to detect and monitor drought in the U.S. Great Plains, U.S.S.R., and Australia during the 1977 crop year. In the U.S., they were able to statistically test their results against results using the Crop Moisture Index (CMI, ref. 18), which is known to detect water stress well, and found the drought test procedure based on the GIN worked very well. In the foreign areas, with no ground truth and CMI data available, they were unable to test their results statistically, however, the U.S. agricultural attaché for the U.S.S.R. verified that the U.S.S.R. regions which were identified as water-stressed by the GIN test had indeed undergone water stress at that time, and also a general moisture condition map produced by the Australian government showed general agreement with GIN test results.

Landsat D, when launched, is scheduled to have thermal infrared bands. It is thought that these bands may prove to be useful in water stress studies since laboratory studies indicate strong water absorption of irradiance in the 1.2 - 2.5 μm wavelengths (ref. 6, page 16-4; ref. 7, page 2-3).

Research in the area of nutrient deficient crops has not yet reached the point of using any of the common Landsat VINs (not counting individual band VINs). However, many results have been obtained which are useful to know and certainly will affect future Landsat research and design of new Landsat systems.

Much of the study on crop nutrient deficiency has been done with corn. Al-Abbas et al. (ref. 2) conducted a study using nitrogen-, phosphorus-, potassium-, sulfur-, magnesium-, and calcium-deficient corn leaves along with a control group of normal corn leaves. He found that the chlorophyll concentration in all nutrient-deficient leaves was lower than that of the normal leaves. He also found that in the near-infrared wavelengths leaves from the phophorus-and calcium deficient plants absorbed more energy than those from normal plants whereas leaves from the sulfur-, magnesium-, potassium-, and nitrogen-deficient plants absorbed less.

Bauer (ref. 5, page 6) studied nitrogent-deficient corn versus normal corn and found nitrogen deficiency caused increased reflectance in the visible wavelengths and decreased reflectance in the near-infrared wavelengths.

Cate, Artley, and Phinney (ref. 7, pages 4-2, and 4-3) report that nitrogen deficiency has been found to increase leaf reflectance in the visible bands in cotton, cabbage, and sweet peppers also. This same report also includes discussion on more nutrient deficiency studies involving mexican squash and sorghum.

The use of Landsat in diseased or infested crop research appears to be pretty dim for at least the immediate future, although again there has been research which will affect future Landsat research and design. Studies conducted by Ausmus and Hilty (ref. 4) and Bauer (ref. 5, page 6) suggest that the near-infrared wavelengths (0.8 - 2.6 μm) were helpful in southern corn blight detection. Other studies (see ref. 7, page 4-5) also indicate that near-infrared bands may be useful in disease detection. The launching of Landsat D should help out in this area; however, Heller (ref. 9) advises that Landsat bands need to be both narrower and more selective in both the visible and near-infrared wavelengths to effectively detect vegetation damage, whether it be caused by disease or insect-infestation. A major "new" Landsat band suggested by Heller is a 0.58 - 0.62 band (a narrow yellow-orange band considered very useful for vegetation damage assessment).

Disease and insect-infestation trends can be identified and monitored now by use of remote sensing, according to Heller (ref. 9, page 1159), but require a series of acquisitions over one or more seasons.

3.3 CROP IDENTIFICATION AND GROWTH STAGE

Using crop calendar knowledge, VIN computations considered over time have been used to help identify general crop types such as spring small grains versus other, winter grains versus other, and summer crops versus other. Ashburn (ref. 3) discusses a major well documented method which has been used in the past and also considers approaches to this problem in general.

Discrimination of specific crops within a general crop type (such as spring wheat versus spring barley) is a further and sometimes difficult problem. For instance, although spring wheat and spring barley have known differences in phenology when grown under identical conditions, in actual cases these differences may be difficult to see due to differences in planting date, stress factors, and other factors.

Any use of a VIN approach for general or specific crop identification depends, of course, on knowledge of growth stage. Aaronson and Davis (ref. 1, page 11), in their comparative study of nine different VINs, note that all VINs have a similar relationship to growth stage. The graph below (copied from ref. 1, page 12) depicts this general relationship.

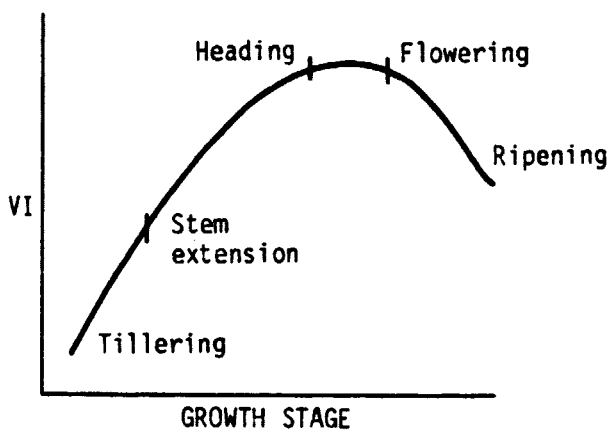

4. SUMMARY

This report was intended to provide some introduction, history, conceptual and mathematical principles, and uses of the more commonly used Landsat vegetative indices of today. Listed on the next page are the VINs considered in this report.

LANDSAT VINS

$$AVI = 2(CH4) - CH2$$

$$DVI = 2.4(CH4) - CH2$$

$$GVI = -.283(CH1) - .660(CH2) + .577(CH3) + .388(CH4)^*$$

$$SBI = .332(CH1) + .603(CH2) + .676(CH3) + .263(CH4)^*$$

$$KVI = GVI - (\text{Soil Line Calculation})$$

$$LAI = 2.677 - 3.698\left(\frac{CH1}{CH2}\right) - 2.309\left(\frac{CH1}{CH3}\right) + 5.751\left(\frac{CH1}{2CH4}\right) + .043\left(\frac{CH2}{CH3}\right)$$

$$-2.692\left(\frac{CH2}{2CH4}\right) + 3.071\left(\frac{CH1}{CH2} - \frac{CH1}{2CH4}\right)\left(\frac{CH1}{CH2}\right)$$

$$PVI6 = \sqrt{[-.498 - .457(CH2) + .498(CH3)]^2 + [2.734 + .498(CH2) - .543(CH3)]^2}$$

$$PVI7 = \sqrt{[.355(CH4) - .149(CH2)]^2 + [.355(CH2) - .852(CH4)]^2}$$

$$TVI6 = \sqrt{\frac{CH3 - CH2}{CH3 + CH2} + 0.5}$$

$$TVI7 = \sqrt{\frac{CH4 - CH2}{CH4 + CH2} + 0.5}$$

*For standard Landsat 2

5. BIBLIOGRAPHY

1. Aaronson, A. C.; and Davis, L. L.: An Evaluation of Relationships between Vegetative Indices, Soil Moisture and Wheat Yields. Crop Condition Assessment Division, Foreign Agricultural Service (9-TM, Sept. 17, 1979).

2. Al-Abbas, A. H.; Barr, R.; Hall, J. D.; Crane, F. L.; and Baumgardner, M. F.: Spectra of Normal and Nutrient-Deficient Maize Leaves. Agronomy Journal, vol. 66, 1974, pp. 16-20.

3. Ashburn, P.: The Vegetative Index Number and Crop Identification. The LACIE Symposium, July 1979, pp. 843-855.

4. Ausmus, F.; and Hilty, I. W.: Reflectance Studies of Healthy, Maize Dwarf Mosaic Virus-Infected, and Helminthosporium maydis-Infected Corn Leaves. Remote Sensing of Environment, vol. 2, 1972, pp. 77-81.

5. Bauer, M. E.: Spectral Characteristics and Remote Sensing of Corn and Soybeans. Proceedings of the 1978 LACIE Corn-Soybean Seminar, JSC-13744, 1978, pp. 3-24.

6. Blad, B. L.: Application of Remote Sensing of the Estimation of Evapotranspiration. Proceedings of the 1974 Lyndon B. Johnson Space Center Wheat Yield Conference, JSC-09256, NASA TM X-58158, 1974, pp. 16-1 to 16-8.

7. Cate, R. B.; Artley, J. A.; and Phinney, D. E.: Quantitative Estimation of Plant Characteristics Using Spectral Measurement — A Survey of the Literature. AgRISTARS Technical Report, JSC-16298, SR-L0-00408, LEMSCO-14077, January 1980.

8. Cicone, R.; Crist, E.; Kauth, R.; Lambeck, P.; Manila, W.; and Richardson, W.: Development of Procedure M for Multicrop Inventory with Tests of a Spring-Wheat Configuration. ERIM 132400-16-F, March 1979, NASA Contract No. NAS9-15476, pp. 40-43.

9. Heller, R. C.: Case Applications of Remote Sensing for Vegetation Damage Assessment. Photogrammetric Engineering and Remote Sensing, vol. 44, no. 9, September 1978, pp. 1159-1166.

10. Kanemasu, E. T.: Estimated Winter Wheat Yield from Crop Growth Predicted by Landsat. Kansas Evapotranspiration Laboratory (Manhattan), Final Report for Period April 1977 to December 1978, NASA Contract NAS9-14899-3S.

11. Kanemasu, E. T.: Seasonal Canopy Reflectance Patterns of Wheat, Sorghum, and Soybean. Remote Sensing of Environment, vol. 3, 1974, pp. 43-47.

12. Kauth, R. J.; Lambeck, P. F.; Richardson, W.; Thomas, G. S.; and Pentland, A. P.: Feature Extraction Applied to Agricultural Crops as Seen by Landsat. The LACIE Symposium, July 1979, pp. 705-721.

13. Kauth, R. J.; and Thomas, G. S.: The Tasselled Cap — A Graphic Description of the Spectral Temporal Development of Agricultural Crops as Seen by Landsat. Proceedings of the Symposium on Machine Processing of Remote Sensing Data. Laboratory for the Applications of Remote Sensing of Purdue Univ., 1976, pp. 4B-41 to 4B-51.

14. Pearson, R. L.; and Miller, L. D.: Remote Mapping of Standing Crop Biomass for Estimation of the Productivity of the Shortgrass Prairie, Pawnee National Grasslands, Colorado. Proceedings of the Eighth International Symposium on Remote Sensing of the Environment, Univ. of Michigan, Willow Runs Labs. (Ann Arbor), 1973, pp. 1355-1381.

15. Potter, J. F.: The Correction of Landsat Data for the Effects of Haze, Sun Angle, and Background Reflectance. Proc. Symposium on Machine Processing of Remotely Sensed Data, (West Lafayette, IN), 1977, pp. 24-32.

16. Richardson, A. J.; and Wiegand, C. L.: Distinguishing Vegetation from Soil Background Information. Photogrammetric Engineering and Remote Sensing, vol. 43, no. 12, December 1977, pp. 1541-1552.

17. Rouse, J. W.; Haas, R. H.; Schell, J. A.; and Deering, D. W.: Monitoring Vegetation Systems in the Great Plains with ERTS. Third ERTS Symposium (Washington, D.C.), NASA SP-351, December 1973, I: 309-317.

18. Sadowski, A.: Crop Moisture Index. Technical Procedures Bulletin 13, U.S. Dept. of Commerce, 1975.

19. Tappan, G.: The Monitoring of Rangeland Vegetation Cover in the Kansas Flint Hills from Landsat Data. Master's Thesis, Univ. of Kansas at Lawrence, 1980, 104 pps.

20. Thompson, D. R.; and Wehmanen, O. A.: Using Landsat Digital Data to Detect Moisture Stress. Photogrammetric Engineering and Remote Sensing, vol. 45, no. 2, 1979, pp 201-207.

21. Wiegand, C. L.; Richardson, A. J.; and Kanemasu, E. T.: Leaf Area Index Estimates for Wheat from Landsat and Their Implications for Evapotranspiration and Crop Modeling. Agronomy Journal, vol. 71, 1979, pp. 336-342.